

A Appendix

In this section, we include related proofs, additional simulation plots that demonstrate the necessity of our proposed debiased causal tree, and a brief introduction to our Supplementary materials.

A.1 Related Proofs

Proof of Theorem 1 By the triangular inequality, we obtain

$$\begin{aligned} |\eta(x) - \eta^*(x)| &\leq \sum_{j=1}^q |\delta_{t_m}(Q_j^{**}) - \eta^*(Q_j^{**})| \mathbb{I}\{x \in Q_j^{**}\} + \sum_{j=1}^q |\eta^*(Q_j^{**}) - \eta^*(x)| \mathbb{I}\{x \in Q_j^{**}\} \\ &\leq \sum_{j=1}^q |\mathbf{b}_{t_m}(Q_j^{**})| \mathbb{I}\{x \in Q_j^{**}\} + \max_{1 \leq j \leq q} \sup_{x \in Q_j^{**}} |\eta^*(Q_j^{**}) - \eta^*(x)|. \end{aligned} \quad (15)$$

By the Cauchy–Schwarz inequality, we further obtain

$$\sum_{j=1}^q |\mathbf{b}_{t_m}(Q_j^{**})| \mathbb{I}\{x \in Q_j^{**}\} \leq \left\{ \sum_{j=1}^q |\mathbf{b}_{t_m}(Q_j^{**})|^2 \right\}^{1/2}. \quad (16)$$

Next, we bound $\sum_{j=1}^q |\mathbf{b}_{t_m}(Q_j^{**})|^2 = \exp\{B(t_m)\}$. By Assumption 2, it holds that

$$B(t_m) \leq B(t_k) + L|t_m - t_k|, \quad \text{i.e.,} \quad \sum_{j=1}^q |\mathbf{b}_{t_m}(Q_j^{**})|^2 \leq e^{L|t_m - t_k|} \sum_{j=1}^q |\mathbf{b}_{t_k}(Q_j^{**})|^2,$$

which implies that

$$\sum_{j=1}^q |\mathbf{b}_{t_m}(Q_j^{**})|^2 \leq e^{L(t_m - t_1)} \frac{1}{m-1} \sum_{k=1}^{m-1} \sum_{j=1}^q |\mathbf{b}_{t_k}(Q_j^{**})|^2. \quad (17)$$

Choosing $C_L \equiv e^{L(t_m - t_1)}$, and combining (15)–(17) give

$$\sup_{x \in [0,1]^p} |\eta(x) - \eta^*(x)| \leq \left\{ \frac{C_L}{m-1} \sum_{k=1}^{m-1} \sum_{j=1}^q |\mathbf{b}_{t_k}(Q_j^{**})|^2 \right\}^{1/2} + \max_{1 \leq j \leq q} \sup_{x \in Q_j^{**}} |\eta^*(x) - \eta^*(Q_j^{**})|.$$

□

Proof of Proposition 1 By (10), under the Gaussian specification of working densities,

$$\hat{\mathbf{H}}(\mathbf{Q}) = \sum_{j=1}^q \left\{ 2(\hat{\theta}_{t,j}^{(0)} - \hat{\theta}_{t,j}^{(1)})^2 + \sum_{i: X_i \in Q_j} \left\{ \frac{D_i(Y_{i,t} - \hat{\theta}_{t,j}^{(1)})^2}{|\{i : X_i \in Q_j, D_i = 1\}|} + \frac{(1 - D_i)(Y_{i,t} - \hat{\theta}_{t,j}^{(0)})^2}{|\{i : X_i \in Q_j, D_i = 0\}|} \right\} \right\}.$$

Under the unconfoundedness condition, if $Y_{i,t} \sim Y_t$ with mean μ_t and variance σ_t^2 independently, for each given Q_j ,

$$\hat{\theta}_{t,j}^{(d)} = \sum_{i=1}^n \frac{Y_{i,t} \mathbb{I}\{D_i = d, X_i \in Q_j\}}{n_d(Q_j)}, \quad \text{where} \quad n_d(Q_j) = |\{i : X_i \in Q_j, D_i = d\}|,$$

is the mean of i.i.d random variables with finite second moment and $\hat{\theta}_{t,j}^{(0)}$ is independent of $\hat{\theta}_{t,j}^{(1)}$. Thus,

$$E[(\hat{\theta}_{t,j}^{(0)} - \hat{\theta}_{t,j}^{(1)})^2] = \sigma_t^2 \left(\frac{1}{n_1(Q_j)} + \frac{1}{n_0(Q_j)} \right),$$

and

$$E \left[\sum_{i: X_i \in Q_j} \left\{ \frac{D_i(Y_{i,t} - \hat{\theta}_{t,j}^{(1)})^2}{|\{i : X_i \in Q_j, D_i = 1\}|} + \frac{(1 - D_i)(Y_{i,t} - \hat{\theta}_{t,j}^{(0)})^2}{|\{i : X_i \in Q_j, D_i = 0\}|} \right\} \right] = \sigma_t^2 \left(\frac{n_1(Q_j) - 1}{n_1(Q_j)} + \frac{n_0(Q_j) - 1}{n_0(Q_j)} \right).$$

We then conclude that

$$E[\hat{\mathbf{H}}(\mathbf{Q})] = 2\sigma_t^2 + \sigma_t^2 \sum_{j=1}^q \frac{n_0(Q_j) + n_1(Q_j)}{n_0(Q_j)n_1(Q_j)}.$$

□

A.2 Additional Simulation Plots

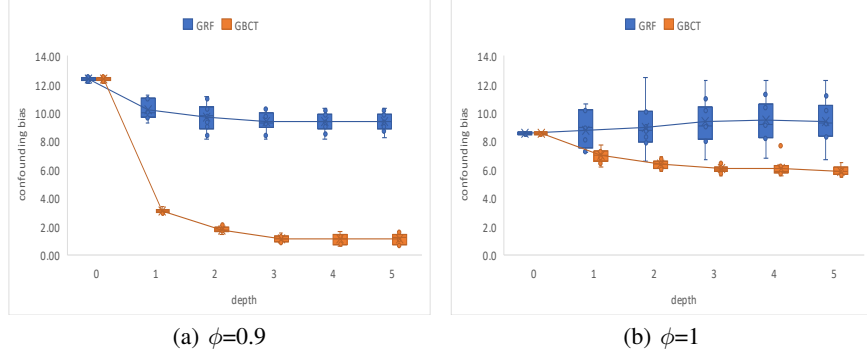


Figure 1: The confounding bias on the validation data under different depths of a single causal tree in the unmeasured confounding scenario. The y -axis represents the empirical confounding bias $\sum_{j=1}^{q_1} |\hat{b}_{t_m}(\hat{Q}_j)|$, where $\{\hat{Q}_j\}_j$ denotes the partition of a single tree in GRF or GBCT and \hat{b}_{t_m} is defined in Eq. 7. The x -axis represents the depth of the causal tree. The data are generated in the same way as described in Section 4. The results show that GBCT performs better than GRF at the single-tree scale in reducing confounding bias.

A.3 Introduction to Supplementary Materials

Supplementary materials contain a more formal version of our response to official reviews from three anonymous referees and implementation details (including codes) of the data generating process in this paper.